

# Superconductivity in the Bilayer Two-orbital Hubbard Model

Yao-Yuan Zheng and Wéi Wú\*

School of Physics, Sun Yat-sen University, Guangzhou, Guangdong 510275, China

(Dated: December 7, 2023)

Motivated by the recently discovered high  $T_c$  nickelate superconductor  $\text{La}_3\text{Ni}_2\text{O}_7$ , we investigate superconductivity in a two dimensional Hubbard model on square lattice that consists of two layers of hybridizing  $d_{x^2-y^2}$  and  $d_{z^2}$  orbitals. Employing cluster dynamical mean-field theory, we establish phase diagrams resolving the crucial dependence of superconducting  $T_c$  on electron hybridization  $V$  between the  $d_{x^2-y^2}$  and  $d_{z^2}$  orbitals at the same layer, and on the vertical hopping  $t_\perp$  between two  $d_{z^2}$  orbitals at different layers.  $V$  and  $t_\perp$  are presumably linked to the pairing phase coherence, and the “pairing glue” of the system respectively. Our result favors a two-component theory explanation of superconductivity in a composite system. The influence of the pseudogap effect and Hund’s coupling on superconductivity are discussed, and also the implication of our result to the understanding of  $\text{La}_3\text{Ni}_2\text{O}_7$  superconductivity.

*Introduction* - Since the discovery of heavy fermion and cuprate superconductors [1, 2], unraveling unconventional superconductivity (SC) [3–11] has been one of the thematic topics in condensed matter physics. For cuprates, despite the precise nature of  $d$ -wave pairing remains a mystery, it is generally believed that the short-ranged antiferromagnetic (AFM) correlations [11–13] lie at the heart of SC, which may be essentially captured by the single-band Hubbard model or the  $t - J$  model encoding the correlation effects of the  $\text{Cu-}3d_{x^2-y^2}$  electrons [6, 8]. It is worth noting that, many other superconductors, including the layered organic superconductor [14] and the transition metal dichalcogenides (TMDs) [15], can also be described by the single-band Hubbard model.

Very recently, novel high  $T_c$  superconductivity is reported in the pressurized nickelate  $\text{La}_3\text{Ni}_2\text{O}_7$  [3, 16–22], which has a layered structure consisting of double  $\text{NiO}_2$  planes. As revealed by the density functional theory (DFT) calculations [23–28] and experiments [29], the  $e_g$  doublet of  $\text{Ni-}3d$  orbitals, *i.e.*, the  $3d_{x^2-y^2}$  and  $3d_{z^2}$  orbitals are both at play in low-energy physics. The  $d_{z^2}$  orbital can be seen as more localized and near half-filled, whereas the  $d_{x^2-y^2}$  orbital is near quarter-filling and in general, more itinerant [30, 31]. Electrons at two different  $e_g$  orbitals can hybridize via an intra-layer hopping  $V$  between them. The out-of-plane electron hopping  $t_\perp$  between  $d_{z^2}$  orbitals at two different  $\text{NiO}_2$  layers, generates an effective AFM coupling  $J_\perp$  deemed to be the major source of the correlation effects in the system (see Fig. 1) [31–33]. The above picture can be in general summarized as a bilayer two-orbital model [24] of  $\text{La}_3\text{Ni}_2\text{O}_7$ , which differs essentially from the Hubbard model of cuprates, or that of the infinite layer nickelates  $R\text{NiO}_2$  ( $R=\text{La,Pr,Ni}$ ) [34] which to be captured by  $d_{x^2-y^2}$  orbital hybridizing with the less correlated  $5d$ -derived bands [35–38]. It is also argued that the Hund’s coupling  $J_H$  may play an important role in  $\text{La}_3\text{Ni}_2\text{O}_7$  [39–41].

All in all, the low-energy physics of  $\text{La}_3\text{Ni}_2\text{O}_7$  could

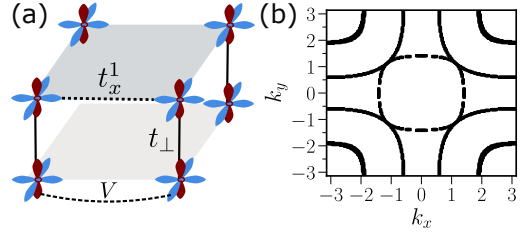


FIG. 1. Geometry and Fermi surface of the bilayer two-orbital Hubbard model. In subplot (a) the light symbols denote  $d_{x^2-y^2}$  orbitals while dark symbols denote  $d_{z^2}$  orbitals. To plot the Fermi surface in subplot (b),  $t_x^1 = -1, t_x^2 = 0.15, t_z^1 = -0.25, t_z^2 = -0.05, \mu_x = -1.6, \mu_z = -0.8, t_\perp = 1.3, V = 0.5$  are used.

be sharply distinguished from previously known unconventional superconductors. A systematic study of SC in the bilayer two-orbital Hubbard (BLTO-Hubbard) model will not only shed light on comprehending  $\text{La}_3\text{Ni}_2\text{O}_7$  superconductivity, but also provide new insights into the general understanding of unconventional superconductivity.

In this work, we investigate superconductivity in BLTO-Hubbard model using cluster extensions of the dynamical mean-field theory (DMFT) [42, 43]. Performing finite temperature computations, we reveal following key aspects of SC in this system: (1) The  $s \pm$ -wave pairing [44–54] driven by inter-layer AFM coupling between  $d_{z^2}$  orbitals with effective  $J_\perp \propto t_\perp^2/U_z$ , has a non-monotonic dependence on  $t_\perp$ . In small  $t_\perp$  regime, superconducting  $T_c$  grows with  $t_\perp$  (or  $J_\perp$ ), whereas at large  $t_\perp$ ,  $T_c$  can be suppressed by increasing  $t_\perp$  (or  $J_\perp$ ). Here  $U_z$  is the Hubbard repulsion within  $d_{z^2}$  orbital. (2) There exists a critical  $V_c$  only when the  $d_{z^2}$ - $d_{x^2-y^2}$  hybridization  $V$  greater than which the system can be superconducting. The relation between  $V$  and phase coherence of pairing is discussed. (3) The superconducting  $T_c$  for the parameters in close relevance to pressurized  $\text{La}_3\text{Ni}_2\text{O}_7$  is estimated as  $\sim 100$  Kelvins, in agreement with the experimental value  $T_c \approx 80\text{K}$  [3]. Increasing  $V$  leads to higher

superconducting  $T_c$ . Finally, we show that the Hubbard repulsion  $U_x$  within the itinerant  $d_{x^2-y^2}$  orbital, as well as a moderate longitudinal Hund's coupling  $J_H$ , do not essentially alter SC in this model. The connection between our result and the two-component theory of superconductivity in a composite system [55–57] is discussed.

*Model and method* - The bilayer two-orbital Hubbard model [24] we use can be written as  $H = H_0 + H_U$ , which reads,

$$H_0 = -t_x^{ij} \sum_{ij\alpha\sigma} c_{i\alpha\sigma}^\dagger c_{j\alpha\sigma} - t_z^{ij} \sum_{ij\alpha\sigma} d_{i\alpha\sigma}^\dagger d_{j\alpha\sigma} - t_\perp \sum_{i\sigma\alpha} d_{i\alpha\sigma}^\dagger d_{i\bar{\alpha}\sigma} + V \sum_{\langle ij \rangle \alpha \sigma} c_{i\alpha\sigma}^\dagger d_{j\alpha\sigma} - \mu_x \sum_{i,\alpha,\sigma} n_{i\alpha\sigma}^x - \mu_z \sum_{i,\alpha,\sigma} n_{i\alpha\sigma}^z \quad (1)$$

$$H_U = U_z \sum_{i\alpha} n_{i\alpha\uparrow}^z n_{i\alpha\downarrow}^z \quad (2)$$

where  $t_x^{ij}$ ,  $t_z^{ij}$  are the in-plane (or intra-layer) intra-orbital electron hoppings for  $d_{x^2-y^2}$  and  $d_{z^2}$  orbitals respectively.  $\alpha$  enumerates the two layers ( $\alpha = 1, 2$ ) and  $\sigma$  indicates spin up/down. We set the in-plane hopping between nearest neighbor (NN) sites of  $d_{x^2-y^2}$  orbitals  $t_x^1 \equiv t = 1$  as the energy unit throughout the work. According to DFT downfolding [24],  $t_x^1 \sim 0.5eV$ , following which the in-plane next-nearest neighbor (NNN) hopping of  $d_{x^2-y^2}$  orbitals is taken as  $t_x^2 = 0.15t$ . For the in-plane hopping of  $d_{z^2}$  orbitals, NN hopping  $t_z^1 = -0.25$ , and NNN hopping  $t_z^2 = -0.05$ . The orbital energies  $\mu_x$  and  $\mu_z$  are used to adjust the fillings of the two orbitals [31], while the total filling of  $e_g$  sub-shell,  $n_z + n_x = 0.75$  is fixed. The hybridization between  $d_{z^2}$  and  $d_{x^2-y^2}$  orbital at the same layer  $V$ , as well as the hopping  $t_\perp$  between two  $d_{z^2}$  orbitals at the same site but different layers, will be the main controlling parameters in our study (see also Fig.1).

For the interacting part  $H_U$ , we will first consider only the Hubbard repulsion  $U_z = 7$  between the  $d_{z^2}$  electrons, the more itinerant  $d_{x^2-y^2}$  orbital will be taken as non-interacting. In the end of the work, the Hubbard repulsion within  $d_{x^2-y^2}$  orbital  $U_x$ , inter-orbital Hubbard  $U_{xz}$ , as well as a longitudinal Hund's coupling  $J_H$  will be considered.

The cluster DMFT methods have been extensively used in studying cuprates and related problems for they can effectively capture temporal and short-ranged spatial correlations [43, 58]. Depending on the boundary conditions of the effective cluster, there can be dynamical cluster approximation (DCA) and cellular DMFT (CDMFT) variations [43]. As we will show below, our results using different clusters converge rapidly against cluster size, demonstrating unambiguously the solidness of the cluster DMFT methods on computing  $T_c$  in this system. We will use the continuous time quantum Monte Carlo (CTQMC) [59] as impurity solver. For cases with

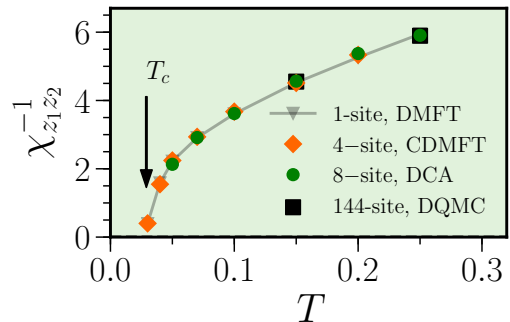


FIG. 2. Inverse of the inter-layer  $d_{z^2} - d_{z^2}$  component of the  $s_\pm$ -wave pairing susceptibility,  $[\chi_{z1,z2}]^{-1}$  as a function of temperature  $T$ . The temperature where  $[\chi_{z1,z2}]^{-1} \rightarrow 0$  is defined as the superconducting transition  $T_c$ . Here  $U_z = 7$ ,  $n_z = 0.47$ ,  $n_x = 0.28$ ,  $t_\perp = 0.8$ ,  $V = 0.5$ . HFQMC impurity solver is used here.

severe sign problem, as will be explicitly stated, Hirsch-Fye quantum Monte Carlo (HFQMC) impurity solver is also used. We have carefully verified that the two impurity solvers give the same result. Determinant quantum Monte Carlo (DQMC) is also employed to benchmark our cluster DMFT result at high temperatures.

*Pairing susceptibility*- For a multi-band system, different components of the pairing susceptibility can simultaneously diverge as approaching superconducting  $T_c$  [60]. Without loss of generality, here we select a  $d_{z^2}$  component of the pairing susceptibility,  $\chi_{z1,z2}$ , in which we find the dominant branch of the  $s_\pm$  wave pairing (see discussion below), to identify the pairing  $T_c$ ,

$$\chi_{z1,z2} = \frac{1}{N} \sum_{i,j} \int_0^\beta \langle \mathcal{T}_\tau p_j^\dagger(\tau) p_i(0) \rangle d\tau \quad (3)$$

where  $p_i$  is the on-site inter-layer spin-singlet pairing operator  $P_i = 1/\sqrt{2}(d_{i,1,\uparrow}d_{i,2,\downarrow} - d_{i,1,\downarrow}d_{i,2,\uparrow})$  of the  $d_{z^2}$  orbital. Fig. 2 plots the inverse pairing susceptibility  $\chi_{z1,z2}^{-1}$  as a function of temperature  $T$  for  $d_{z^2}$ ,  $d_{x^2-y^2}$  orbital being respectively close to half-, and quarter-filling ( $n_z \sim 0.5$ ,  $n_x \sim 0.25$ ). One sees that as lower temperature  $T$ ,  $\chi_{z1,z2}^{-1}$  decreases and eventually extrapolates to zero as approaching  $T_c \sim 0.029$  (black arrow), indicating the occurrence of spontaneous instability of SC in this system. In Fig. 2, we find that different cluster DMFT schemes, including the single-site ( $1 \times 4$  orbitals) DMFT, four-site ( $4 \times 4$  orbitals) CDMFT, and eight-site ( $8 \times 4$  orbitals) DCA, all give results in excellent agreement with one another, which are agreed by the 144 site ( $12 \times 12 \times 4$  orbitals) DQMC simulations at  $T = 0.25, 0.15$ . This result demonstrates that the non-local fluctuations are insignificant in the BLTO-Hubbard model for the given parameters, and also indicates the reliability of our cluster DMFT results on  $T_c$  in this study. This observation

is in contrast to the case of single-band Hubbard model of cuprates, where finite-site effects are typically strong in small DCA clusters [58].

Further decreasing temperature  $T$ , one obtains finite SC order parameter  $\Delta_{ij}^{\alpha,\beta} = \langle \phi_{i\alpha\uparrow}^\dagger \phi_{j\beta\downarrow}^\dagger \rangle$ ,  $\phi_{i\alpha\sigma} \in \{c_{i\alpha\sigma}^\dagger, d_{i\alpha\sigma}^\dagger\}$  in real space when  $T < T_c$ . As shown in Table I, we find that the local inter-layer ( $R_i = R_j, \alpha \neq \beta$ ) components overweight all other non-local ( $R_i \neq R_j$ ) branches, suggesting that the SC can be best described as an  $s_{\pm}$ -wave pairing here, which agrees with previous studies [44, 45, 47–50, 61].

*Phase diagram*- We now study the dependence of  $T_c$  on the inter-layer  $d_{z^2}$ - $d_{z^2}$  hopping  $t_{\perp}$ . In the localized and large  $U_z$  limit of  $d_{z^2}$  orbital, the effective AFM exchange  $J_{\perp}$  between the two  $d_{z^2}$  orbitals scales like  $J_{\perp} \sim t_{\perp}^2/U_z$  to dominant order. As found in cuprates [11, 62], one may expect that the superconducting  $T_c$  would grow with magnetic coupling  $J_{\perp}$ , or equivalently with  $t_{\perp}$  here. This is indeed what we observe in the small  $t_{\perp}$  regime in Fig. 3, where results for two different dopings,  $n_z = 0.47$  (squares) and  $n_z = 0.45$  (diamonds) are shown. At large  $t_{\perp}$ , saying  $t_{\perp} \gtrsim 0.8$  for  $n_z = 0.47$ , we however find that  $T_c$  decreases as increasing  $t_{\perp}$ . In other words, non-monotonic dependence of  $T_c$  on  $t_{\perp}$  (or  $J_{\perp}$ ) is observed in Fig. 3, which appears to resemble the BCS-BEC crossover phase diagram [63]. To gain insight into this observation, the Inset of Fig. 3 compares the imaginary part of the local Green's function of the  $d_{z^2}$  orbital  $-\text{Im}G_{z_1 z_1}(i\omega_n)$  for two different  $t_{\perp}$  at  $n_z = 0.47$ . As one can see that at large  $t_{\perp}$  ( $t_{\perp} = 1.0$ ), the low-energy weight of the Green's function in the normal state ( $T = 0.04 > T_c$ ) is greatly suppressed comparing to the smaller  $t_{\perp} = 0.4$  case. Further analysis indicates that the suppression of Green's function in the normal state at  $t_{\perp} = 1.0$  corresponds to the opening of a pseudogap in the low-energy density of states (not shown here). Verifying whether the BCS-BEC crossover theory applies in this model requires identifying the physical origin of the pseudogap, which can be done, for example, by using the fluctuation diagnostics method [64, 65] in future studies. It is worth noting that in cuprate, it is generally believed that the SC state is far from the BEC limit [66], despite the existence of pseudogap. Summarizing Fig. 3, we find the tendency that as  $n_z$  decreases, the suppression of the low-energy local

$\langle d_{i,z_1\uparrow}^\dagger d_{i,z_2\downarrow}^\dagger \rangle$	$\langle c_{i,x_1\uparrow}^\dagger c_{i,x_2\downarrow}^\dagger \rangle$	$\langle d_{i,z_1\uparrow}^\dagger d_{i+1,z_1\downarrow}^\dagger \rangle$	$\langle c_{i,x_1\uparrow}^\dagger c_{i+1,x_1\downarrow}^\dagger \rangle$
0.010	0.013	0.002	0.0003

TABLE I. Superconducting order parameter in real-space at  $U_z = 7, n_z = 0.47, n_x = 0.28, t_{\perp} = 0.8, V = 0.5$  (same as in Fig. 2) from 4-site ( $2 \times 2$ ) CDMFT,  $T = 0.025 < T_c \approx 0.029$ . Here  $\langle d_{i,z_1\uparrow}^\dagger d_{i,z_2\downarrow}^\dagger \rangle$  is the on-site, inter-layer,  $d_{z^2}$  orbital component of SC order parameter, while  $\langle c_{i,x_1\uparrow}^\dagger c_{i+1,x_1\downarrow}^\dagger \rangle$  denotes the  $d_{x^2-y^2}$  orbital component on the intra-layer nearest neighbor bond. HFQMC solver is used here.

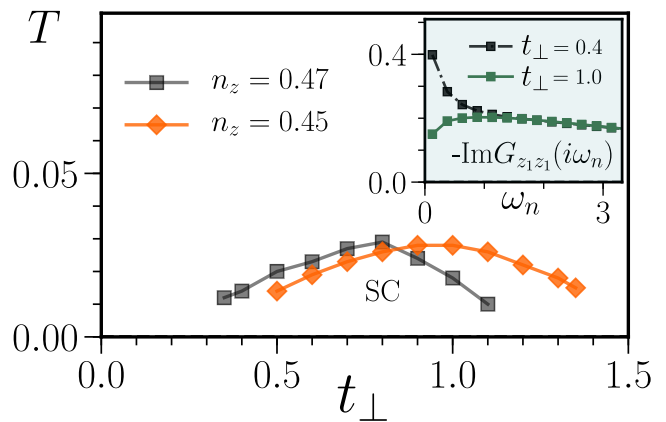


FIG. 3. Superconducting transition temperature  $T_c$  as a function of the vertical hopping amplitude  $t_{\perp}$  between two inter-layer  $d_{z^2}$  orbitals. Results for two different dopings are shown. **Inset:** Imaginary part of the local Green's function of  $d_{z^2}$  orbital  $-\text{Im}G_{z_1 z_1}(i\omega_n)$  are shown as a function of Matsubara frequency  $\omega_n$  for  $n_z = 0.47$  at two different  $t_{\perp}$ . Here  $V = 0.5, U_z = 7, n_x = 0.75 - n_z$ .

Green's functions at large  $t_{\perp}$  becomes less severe, and the dome-like superconducting regime as a whole moves to the large  $t_{\perp}$  side.

Now we focus on the impact of the  $d_{z^2}$ - $d_{x^2-y^2}$  hybridization  $V$  on superconducting  $T_c$ . It is obvious that the SC instability found above cannot be exclusively attributed to the  $d_{z^2}$  orbital alone, although the binding of electrons stems from the effective  $J_{\perp}$  in this orbital. Indeed, here the  $d_{z^2}$  orbital has a small intra-orbital NN hopping  $t_z^{\parallel}/t = -0.25$ , the Cooper pairs face difficulty in propagating coherently within the  $d_{z^2}$  plane to achieve phase ordering. The more itinerant  $d_{x^2-y^2}$  orbital, on the other hand, can boost phase coherence of Cooper pairs via  $d_{z^2}$ - $d_{x^2-y^2}$  hybridization  $V$  [55, 57]. Fig. 4 displays

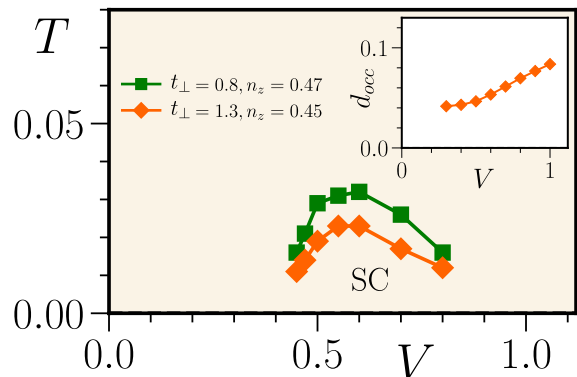


FIG. 4. Superconducting  $T_c$  as a function of  $V$  are shown for two different sets of  $(t_{\perp}, n_z)$  parameters (see also Fig. 3). **Inset:** The double occupancy  $d_{occ} = \langle n_{\uparrow}^d n_{\downarrow}^d \rangle$  of  $d_{z^2}$  orbital as a function of  $V$  at  $(t_{\perp} = 1.3, n_z = 0.45)$ .  $d_{occ}$  increasing with  $V$  suggests the growing itinerancy of  $d_{z^2}$  orbital as  $V$  increases. Here  $U_z = 7, n_x = 0.75 - n_z$ .

superconducting  $T_c$  as a function of  $V$  for two different ( $t_\perp, n_z$ ) parameters. It is clear in Fig.4 that finite  $T_c$  can be obtained only when  $V$  is sufficiently large. Extrapolating  $T_c$  curve to zero  $T$ , taking the  $t_\perp = 0.8$  case for example, a critical  $V_c \sim 0.4$  can be inferred for SC instability in the zero- $T$  limit. As for  $V > V_c$ ,  $T_c$  grows rapidly with  $V$ , which reaches a maximum  $T_c \sim 0.03$  for the  $t_\perp = 0.8$  case. Further increasing  $V$  leads to, nevertheless, a suppression of  $T_c$ . This is because a large  $V$  can delocalize  $d_{z^2}$  electrons, resulting in the disruption of local  $d_{z^2}$  spin singlets and thereby being detrimental to SC. The growing itinerancy of  $d_{z^2}$  electrons with  $V$  can be manifested in the Inset of Fig.4, where the double occupancy  $d_{occ}$  of  $d_{z^2}$  orbital is shown as a function of  $V$ . In Fig. 4, a different parameter set of  $t_\perp = 1.3, n_z = 0.45$  is also shown (diamonds), which exhibits similar  $V$ -dependence of  $T_c$ , suggesting the generality of our analysis above on the role of  $V$ .

It has been proposed by Yang and collaborators [49, 55] that SC in the pressurized  $\text{La}_3\text{Ni}_2\text{O}_7$  fits in a two-component theory. That theory was first established by Kivelson [56, 57] to describe a “composite system” of superconductivity which can be divided into two distinct components: a “pairing” component with high pairing energy scale  $\Delta_0$  but vanishing superfluid stiffness (such as the  $d_{z^2}$  orbital here), and a “metallic” component with no pairing but high superfluid stiffness (like the  $d_{x^2-y^2}$  orbital here). Berg *et al* [57] show that a high  $T_c$  can be reached approaching its mean-field value,  $T_c \sim T_{MF} \approx \Delta_0/2$  if a moderate hybridization between the two components is introduced to suppress the phase fluctuations. In Fig. 2, we indeed see that in the BLTO-Hubbard model the non-local fluctuations beyond the single-site DMFT appear to be unimportant. It is also interesting to notice that here the optimal  $T_c$  is found near hybridization  $V/t \approx (0.55 \sim 0.60)$  for the two parameter sets we study, which coincides with the value  $V/t \sim 0.5$  obtained for the attractive Hubbard model with  $U/t = -1$  [57]. One prominent difference is that, however, we find a finite critical  $V_c \approx 0.4$  for SC, while in Ref. [57] SC vanishes continuously in the  $V \rightarrow 0$  limit. This may be attributed to the temporal fluctuations which are treated exactly in CDMFT here, but absent in the work of Ref. [57].

*Effect of  $U_x, U_{xz}$  and  $J_H$*  - Above we have discussed SC in the BLTO-Hubbard model considering only  $U_z$  [32]. To make closer connection to the realistic materials, other Hubbard parameters, including Hubbard repulsion  $U_x$  within the  $d_{x^2-y^2}$  orbital,  $U_{xz}$  between the  $d_{z^2}$  and  $d_{x^2-y^2}$  orbital on the same site, as well as a longitudinal Hund’s coupling  $J_H$  are considered below as,  $H'_U = U_x \sum_{i\alpha} n_{i\alpha}^x n_{i\alpha\downarrow}^x + U_{xz} \sum_{i\alpha} n_{i\alpha\sigma}^x n_{i\alpha\bar{\sigma}}^z + (U_{xz} - J_H) \sum_{i\alpha,\sigma} n_{i\alpha\sigma}^x n_{i\alpha\sigma}^z$ . In Fig. 6, the inverse pairing susceptibility  $\chi_{z1,z2}^{-1}$  as a function of  $T$  is shown to compare the results with  $H'_U$  included (diamonds), and with-

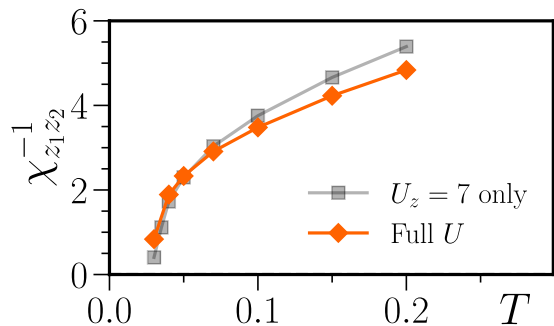


FIG. 5. Inverse pairing susceptibility,  $[\chi_{z1,z2}]^{-1}$  as a function of temperature  $T$  for two different configurations of Hubbard parameters. Full  $U$  denotes the case with  $H'_U$  and  $U_z$  both considered, *i.e.*,  $U_x = U_z = 7, U_{xz} = 5.6, J_H = 0.7$ . HFQMC impurity solver is used here.

out  $H'_U$  (only  $U_z$ , squares). It suggests that including  $H'_U$  ( $U_x, U_{xz}$  and  $J_H$ ) does not change essentially the SC state. The pairing susceptibility  $\chi_{z1,z2}$  is only reduced mildly at low temperatures, indicating a slightly decreased superconducting  $T_c$ . A closer inspection finds that the suppression of  $T_c$  by  $H'_U$  comes mainly from the effects of  $U_x$  and  $J_H$ . We note that a recent numerical study [31] on the more *ab initio* Emery-Hubbard model finds that the Hund’s coupling  $J_H$  plays insignificant role in low-energy physics due to the small filling factor of  $d_{x^2-y^2}$  orbital. A similar conclusion on the role of  $J_H$  is also made by the renormalized mean-field theory study on the bilayer two-orbital  $t - J$  model [50].

*Connection to  $\text{La}_3\text{Ni}_2\text{O}_7$  and raising  $T_c$* - Finally, we discuss the connection between our result and the  $\text{La}_3\text{Ni}_2\text{O}_7$  materials. For pressurized  $\text{La}_3\text{Ni}_2\text{O}_7$ , DFT result suggests  $t_\perp \approx 1.3, V \approx 0.5$  for the BLTO-Hubbard model [24]. However, the Hubbard parameters such as  $U_z$  have not been reliably estimated. In Fig. 6 we therefore plot  $T_c$  as a function  $U_z$  while fixing  $t_\perp = 1.3, V = 0.5$  (squares). As one can see that when  $U_z > 6$ ,  $T_c$  is almost independent of  $U_z$ , suggesting a  $T_c \approx 100$  Kelvin. This result in general agrees with the experimental  $T_c \sim 80K$ . Our study is also consistent with the absence of SC in

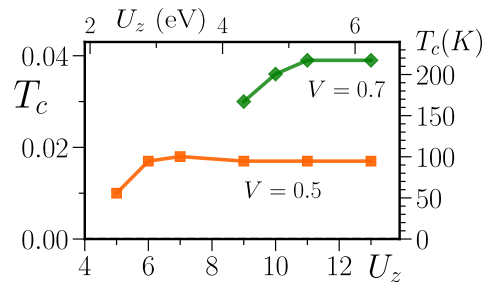


FIG. 6. Superconducting  $T_c$  as a function of  $U_z$  for two different  $V$  at fixed  $t_\perp = 1.3, n_z = 0.45, n_x = 0.3$ . The energy unit  $t_x$  is set as  $t_x^1 = 0.48\text{eV}$  as following the DFT result [24].

$\text{La}_3\text{Ni}_2\text{O}_7$  under ambient pressure where  $d_{z^2}$  orbital is below the Fermi level [30]: the  $d_{z^2}$  orbital is the driving force of the composite SC here. The pairing hence will be disabled if the  $d_{z^2}$  orbital is not active at low-energies. Finally, as shown in Fig 6, we find that  $T_c$  can be considerably enhanced by increasing  $V$ , if  $U_z$  is sufficiently large.

*Discussion and summary* - In cuprates,  $d_{x^2-y^2}$  electrons act concurrently as both carrier and strongly correlated medium where “pairing glue” emerges [67]. The entanglement of the two roles of electrons may be one of the reasons why cuprate SC is so difficult to understand. In pressurized  $\text{La}_3\text{Ni}_2\text{O}_7$ , the two active  $e_g$  orbitals may can be assigned separately to those two different roles for SC. This sheds new light on comprehending unconventional superconductivity from a novel perspective. Future experiments and further theoretical studies on the BLTO-Hubbard model are warranted to confirm whether the two-component theory [55–57] provides a substantial description of the SC in  $\text{La}_3\text{Ni}_2\text{O}_7$ . To summarize, in this work we study superconductivity in the BLTO-Hubbard model by using cluster DMFT methods. We establish phase diagrams revealing the crucial dependence of superconducting  $T_c$  on two key physical parameters,  $V$  and  $t_\perp$  of the system. The relevance of the two-component theory of superconductivity to our results is discussed.

*Acknowledgment*- We thank Meng Wang, A. -M. Tremblay, Dao-Xin Yao, Changming Yue, and Xunwu Hu for useful discussions. W.W is grateful to Guang-Ming Zhang and Yi-feng Yang for discussions and suggestions. Work at Sun Yat-Sen University was supported by the National Natural Science Foundation of China (Grants No.12274472, No.11904413).

---

\* Corresponding author: [wuwei69@mail.sysu.edu.cn](mailto:wuwei69@mail.sysu.edu.cn)

- [1] F. Steglich, J. Aarts, C. Bredl, W. Lieke, D. Meschede, W. Franz, and H. Schäfer, *Physical Review Letters* **43**, 1892 (1979).
- [2] J. G. Bednorz and K. A. Müller, *Zeitschrift für Physik B Condensed Matter* **64**, 189 (1986).
- [3] H. Sun, M. Huo, X. Hu, J. Li, Y. Han, L. Tang, Z. Mao, P. Yang, B. Wang, J. Cheng, D.-X. Yao, G.-M. Zhang, and M. Wang, *Nature* **621**, 493 (2023) (2023).
- [4] F. C. Zhang and T. M. Rice, *Phys. Rev. B* **37**, 3759 (1988).
- [5] P. A. Lee, N. Nagaosa, and X.-G. Wen, *Reviews of Modern Physics* **78**, 17 (2006).
- [6] K. Haule and G. Kotliar, *Physical Review B* **76**, 104509 (2007).
- [7] A. V. Chubukov, D. V. Efremov, and I. Eremin, *Phys. Rev. B* **78**, 134512 (2008).
- [8] D. J. Scalapino, *Reviews of Modern Physics* **84**, 1383 (2012).
- [9] B. Keimer, S. A. Kivelson, M. R. Norman, S. Uchida, and J. Zaanen, *Nature* **518**, 179 (2015).
- [10] X. Zhou, W.-S. Lee, M. Imada, N. Trivedi, P. Phillips, H.-Y. Kee, P. Törmä, and M. Eremets, *Nature Reviews Physics* **3**, 462 (2021).
- [11] N. Kowalski, S. S. Dash, P. Sémon, D. Sénéchal, and A.-M. Tremblay, *Proceedings of the National Academy of Sciences* **118**, e2106476118 (2021).
- [12] B. Keimer, S. A. Kivelson, M. R. Norman, S. Uchida, and J. Zaanen, *Nature* **518**, 179 (2015).
- [13] O. Cyr-Choinière, R. Daou, F. Laliberté, C. Collignon, S. Badoux, D. LeBoeuf, J. Chang, B. Ramshaw, D. Bonn, W. Hardy, *et al.*, *Physical Review B* **97**, 064502 (2018).
- [14] R. H. McKenzie, *Science* **278**, 820 (1997).
- [15] F. Wu, T. Lovorn, E. Tutuc, and A. H. MacDonald, *Phys. Rev. Lett.* **121**, 026402 (2018).
- [16] Z. Liu, H. Sun, M. Huo, X. Ma, Y. Ji, E. Yi, L. Li, H. Liu, J. Yu, Z. Zhang, *et al.*, *Science China Physics, Mechanics & Astronomy* **66**, 217411 (2023).
- [17] Y. Zhang, D. Su, Y. Huang, H. Sun, M. Huo, Z. Shan, K. Ye, Z. Yang, R. Li, M. Smidman, *et al.*, arXiv preprint arXiv:2307.14819 (2023).
- [18] J. Hou, P.-T. Yang, Z.-Y. Liu, J.-Y. Li, P.-F. Shan, L. Ma, G. Wang, N.-N. Wang, H.-Z. Guo, J.-P. Sun, *et al.*, *Chinese Physics Letters* **40**, 117302 (2023).
- [19] J. Li, C. Chen, C. Huang, Y. Han, M. Huo, X. Huang, P. Ma, Z. Qiu, J. Chen, L. Chen, T. Xie, B. Shen, H. Sun, D. Yao, and M. Wang, “Structural transition and electronic band structures in the compressed trilayer nickelate  $\text{La}_4\text{Ni}_3\text{O}_{10}$ ,” (2023), arXiv:2311.16763 [cond-mat.supr-con].
- [20] Q. Li, Y.-J. Zhang, Z.-N. Xiang, Y. Zhang, X. Zhu, and H.-H. Wen, arXiv preprint arXiv:2311.05453 (2023).
- [21] T. Cui, S. Choi, T. Lin, C. Liu, G. Wang, N. Wang, S. Chen, H. Hong, D. Rong, Q. Wang, *et al.*, arXiv preprint arXiv:2311.13228 (2023).
- [22] L. Sun, Y. Zhou, J. Guo, S. Cai, P. Wang, J. Zhao, J. Han, X. Chen, Q. Wu, Y. Ding, *et al.*, arXiv preprint arXiv:2311.12361 (2023).
- [23] V. Pardo and W. E. Pickett, *Phys. Rev. B* **83**, 245128 (2011).
- [24] Z. Luo, X. Hu, M. Wang, W. Wú, and D.-X. Yao, *Phys. Rev. Lett.* **131**, 126001 (2023).
- [25] F. Lechermann, J. Gondolf, S. Bötzel, and I. M. Eremin, arXiv preprint arXiv:2306.05121 (2023).
- [26] Y. Zhang, L.-F. Lin, A. Moreo, T. A. Maier, and E. Dagotto, *Physical Review B* **108**, 165141 (2023).
- [27] B. Geisler, J. J. Hamlin, G. R. Stewart, R. G. Hennig, and P. Hirschfeld, arXiv preprint arXiv:2309.15078 (2023).
- [28] V. Christiansson, F. Petocchi, and P. Werner, *Phys. Rev. Lett.* **131**, 206501 (2023).
- [29] Z. Liu, M. Huo, J. Li, Q. Li, Y. Liu, Y. Dai, X. Zhou, J. Hao, Y. Lu, M. Wang, *et al.*, arXiv preprint arXiv:2307.02950 (2023).
- [30] J. Yang, H. Sun, X. Hu, Y. Xie, T. Miao, H. Luo, H. Chen, B. Liang, W. Zhu, G. Qu, *et al.*, arXiv preprint arXiv:2309.01148 (2023).
- [31] W. Wú, Z. Luo, D.-X. Yao, and M. Wang, arXiv preprint arXiv:2307.05662 (2023).
- [32] Y. Shen, M. Qin, and G.-M. Zhang, *Chinese Physics Letters* (2023).
- [33] S. Rye, N. Witt, and T. O. Wehling, arXiv preprint arXiv:2310.17465 (2023).
- [34] D. Li, K. Lee, B. Y. Wang, M. Osada, S. Crossley, H. R. Lee, Y. Cui, Y. Hikita, and H. Y. Hwang, *Nature* **572**, 624 (2019).

- [35] Z. Wang, G.-M. Zhang, Y.-f. Yang, and F.-C. Zhang, *Phys. Rev. B* **102**, 220501 (2020).
- [36] J. Karp, A. S. Botana, M. R. Norman, H. Park, M. Zingl, and A. Millis, *Physical Review X* **10** (2020), 10.1103/physrevx.10.021061.
- [37] Y. Nomura and R. Arita, Reports on Progress in Physics **85**, 052501 (2022).
- [38] M. Kitatani, L. Si, P. Worm, J. M. Tomczak, R. Arita, and K. Held, *Phys. Rev. Lett.* **130**, 166002 (2023).
- [39] H. Oh and Y.-H. Zhang, arXiv preprint arXiv:2307.15706 (2023).
- [40] C. Lu, Z. Pan, F. Yang, and C. Wu, arXiv preprint arXiv:2307.14965 (2023).
- [41] Z. Liao, L. Chen, G. Duan, Y. Wang, C. Liu, R. Yu, and Q. Si, arXiv preprint arXiv:2307.16697 (2023).
- [42] A. Georges, Reviews of Modern Physics **68** (1996).
- [43] T. Maier, M. Jarrell, T. Pruschke, and M. H. Hettler, *Rev. Mod. Phys.* **77**, 1027 (2005).
- [44] Q.-G. Yang, D. Wang, and Q.-H. Wang, *Phys. Rev. B* **108**, L140505 (2023).
- [45] Y.-H. Tian, Y. Chen, J.-M. Wang, R.-Q. He, and Z.-Y. Lu, arXiv preprint arXiv:2308.09698 (2023).
- [46] Y. Gu, C. Le, Z. Yang, X. Wu, and J. Hu, arXiv preprint arXiv:2306.07275 (2023).
- [47] C. Lu, Z. Pan, F. Yang, and C. Wu, arXiv preprint arXiv:2310.02915 (2023).
- [48] X.-Z. Qu, D.-W. Qu, J. Chen, C. Wu, F. Yang, W. Li, and G. Su, arXiv preprint arXiv:2307.16873 (2023).
- [49] Q. Qin and Y.-f. Yang, *Phys. Rev. B* **108**, L140504 (2023).
- [50] Z. Luo, B. Lv, M. Wang, W. Wú, and D.-X. Yao, arXiv preprint arXiv:2308.16564 (2023).
- [51] H. Sakakibara, N. Kitamine, M. Ochi, and K. Kuroki, arXiv preprint arXiv:2306.06039 (2023).
- [52] Z. Pan, C. Lu, F. Yang, and C. Wu, arXiv preprint arXiv:2309.06173 (2023).
- [53] K. Jiang, Z. Wang, and F.-C. Zhang, arXiv preprint arXiv:2308.06771 (2023).
- [54] J. Chen, F. Yang, and W. Li, arXiv preprint arXiv:2311.05491 (2023).
- [55] Y.-f. Yang, G.-M. Zhang, and F.-C. Zhang, *Phys. Rev. B* **108**, L201108 (2023).
- [56] S. Kivelson, *Physica B: Condensed Matter* **318**, 61 (2002).
- [57] E. Berg, D. Orgad, and S. A. Kivelson, *Phys. Rev. B* **78**, 094509 (2008).
- [58] P. Staar, T. Maier, and T. C. Schulthess, *Phys. Rev. B* **89**, 195133 (2014).
- [59] A. N. Rubtsov, V. V. Savkin, and A. I. Lichtenstein, *Phys. Rev. B* **72**, 035122 (2005).
- [60] W. Wu and A.-M.-S. Tremblay, *Phys. Rev. X* **5**, 011019 (2015).
- [61] X.-Z. Qu, D.-W. Qu, W. Li, and G. Su, arXiv preprint arXiv:2311.12769 (2023).
- [62] W. Ruan, C. Hu, J. Zhao, P. Cai, Y. Peng, C. Ye, R. Yu, X. Li, Z. Hao, C. Jin, X. Zhang, Z.-Y. Weng, and Y. Wang, *Science bulletin* **61**, 1826 (2016).
- [63] Q. Chen, J. Stajic, S. Tan, and K. Levin, *Physics Reports* **412**, 1 (2005).
- [64] O. Gunnarsson, T. Schafer, J. P. LeBlanc, E. Gull, J. Merino, G. Sangiovanni, G. Rohringer, and A. Toschi, *Phys Rev Lett* **114**, 236402 (2015).
- [65] W. Wú, X. Wang, and A.-M. Tremblay, *Proceedings of the National Academy of Sciences* **119**, e2115819119 (2022), <https://www.pnas.org/doi/pdf/10.1073/pnas.2115819119>.
- [66] J. Sous, Y. He, and S. A. Kivelson, *npj Quantum Materials* **8**, 25 (2023).
- [67] T. A. Maier, D. Poilblanc, and D. J. Scalapino, *Phys. Rev. Lett.* **100**, 237001 (2008).